Insights into the impact of a green polar solvent on the properties of polysulfone membranes for gas separation applications

Zuzana Krchňáčková[1], Riyadh Abdekadir Khellouf[1], Dominika Hanušová[1], Pavol Šuly[1], Lukáš Münster[1], Miroslava Dušánková[1], Tomáš Plachý[1], Miroslava Kovářová[1*], Vladimír Sedlařík[1*]

[1]Centre of Polymer Systems, University Institute, Tomas Bata University in Zlin, Trida Tomase Bati 5678, 760 01 Zlin, Czech Republic

* Corresponding author: kovarova@utb.cz

Abstract

Replacing toxic solvents with greener options in the preparation of polymer solutions and subsequent membranes is a matter of importance today. This study focused on the use of methyl 5-(dimethylamino)-2-methyl-5-oxopentanoate (MDMO) as an environmentally-friendly alternative to N-methylpyrrolidone (NMP) for the preparation of thin polysulfone films. The correlation between the thickness of the prepared membranes and the concentration and viscosity of the polymer solutions used was evaluated. Attention was also paid to the presence of residual solvents, which were investigated by Fourier-transform infrared spectroscopy, thermogravimetric analysis, headspace gas chromatography, and dynamic mechanical analysis. Gas permeation measurements were performed for three gases (CO_2, N_2 and O_2) with different kinetic diameters of molecules. Although MDMO proved to be a good solvent for polysulfone, the tested cast films did not exhibit the same gas permeability as membranes prepared from polysulfone solutions based on N-methylpyrrolidone.

Keywords: film, membrane, gas permeation, green solvent, methyl 5-(dimethylamino)-2-methyl-5-oxopentanoate

1. Introduction

Organic solvents play a pivotal role in a wide range of industries. Generally, they are used in product formulation and dilution process. However, this process often results in solvent emissions and the generation of hazardous waste (Lau and Koenig, 2001). The concerns associated with conventional organic solvents are particularly significant in membrane fabrication processes, where large quantities of organic solvents are needed to prepare polymer casting solutions and determine the final membrane structure and performance (Dong et al., 2021).

Polymer membranes are widely used in gas separation technology due to their low cost, simple operation, system compatibility, and high selectivity (Maab and Touheed, 2022). Over the years, membrane technology has been successfully employed for the industrial separation of gases, including CO_2, N_2, O_2, and CH_4. The performance of these membranes strongly depends on the properties of the polymeric material used in their fabrication. Among the various membrane-forming polymers, polysulfones have attracted considerable attention due to their excellent thermal, mechanical, and chemical stability. Polysulfones are amorphous thermoplastics characterized by the presence of sulfone groups within their polymer

backbone, along with aromatic rings and ether or isopropylidene linkages, which contribute significantly to their resistance to heat, oxidation, and chemical degradation. The polysulfone family comprises three major members: polysulfone (PSU), polyethersulfone (PESU), and polyphenylsulfone (PPSU), all of which have been extensively investigated for membrane-based gas separation applications (Yong et al., 2018).

Despite these benefits, the preparation of the PSU membrane requires the use of N-methyl-2-pyrrolidone (NMP) to produce a homogeneous casting solution (Loh et al., 2018; Olifirov et al., 2025; Wang et al., 2002). However, this solvent has already been identified by several health and regulatory organizations as a hazardous substance associated with serious adverse effects, particularly on reproductive health (EPA, 2022; European Chemicals Agency., 2019; Keyte et al., 2022). To overcome these challenges, substantial efforts have been undertaken globally; for instance, the European Union has adopted the Chemicals Strategy for Sustainability (CSS), a promising policy that aims to reduce the use of hazardous chemicals and promote safer, more sustainable alternatives (European Commission, 2020).

Among the potential alternatives, Methyl 5-(dimethylamino)-2-methyl-5-oxopentanoate (MDMO) has attracted significant attention as a substitute for traditional aprotic solvents. MDMO is a dipolar aprotic nitrogen-containing solvent that is non-flammable with a very low vapor pressure, and Hansen solubility parameters comparable to those of NMP. Furthermore, toxicological studies have reported no detectable toxicity even at doses of approximately 1000 mg (kg day)$^{-1}$. These characteristics make MDMO an attractive candidate for greener membrane fabrication, as its low toxicity and very low volatility may reduce occupational exposure risks and solvent emissions during processing (Xie et al., 2020; Paolucci et al., 2020; Sarkar et al., 2022). From a mechanistic perspective, solvent selection plays a pivotal role in membrane fabrication by influencing the configuration and arrangement of polymer chains (Liao et al., 2023). The combination of low toxicity, non-flammability, and very low vapor pressure further supports the potential of MDMO to enhance process safety and reduce environmental impact. Hence, replacing NMP with MDMO may contribute to more sustainable membrane manufacturing processes while maintaining the solvent properties needed for effective polysulfone membrane formation.

The use of MDMO as a solvent for the preparation of polysulfone-based membranes has been investigated in several studies, particularly by Dong et al. (Dong et al., 2018a). Their work focused primarily on porous membranes fabricated for microfiltration and ultrafiltration applications, which demonstrated outstanding separation performance. However, these membranes were reported to suffer from occasional collapse of the structure (Dong et al., 2018a, 2020, 2018b).

Although MDMO has shown considerable potential as a sustainable solvent for the fabrication of porous PSU membranes used in ultrafiltration and water-treatment applications, its applicability to dense gas-separation membranes has not yet been extensively investigated. Therefore, there is still limited understanding of how MDMO affects the structure and gas transport performance of dense polysulfone membranes. While state-of-the-art PSU gas-separation membranes often incorporate advanced features such as surface functionalization, polymer blending, and composite architectures, in the present study, a simple doctor-blade

casting method was employed to prepare dense, non-porous polysulfone (PSU) membranes using MDMO as a green solvent. This work aims to provide insight into the impact of an environmentally safer solvent on the fabrication, structure, and gas transport properties of polysulfone-based gas separation membranes.

2. Materials and methods

2.1 Materials

Polysulfone Ultrason S 6010 NAT (PSU, BAFS SE, Germany), methyl 5-(dimethylamino)-2-methyl-5-oxopentanoate (MDMO, P-LAB, Czech Republic), and N-methylpyrrolidone (NMP, Sigma Aldrich, Germany), were all applied as received. All the gases for the permeation tests were purchased from SIAD (Italy). The chemical structures of the polymer and solvents are shown in Figure 1. Table 1 lists some basic physicochemical properties of the solvents compared (Dong et al., 2018a; Sarkar et al., 2022; SOLVAY, n.d.).

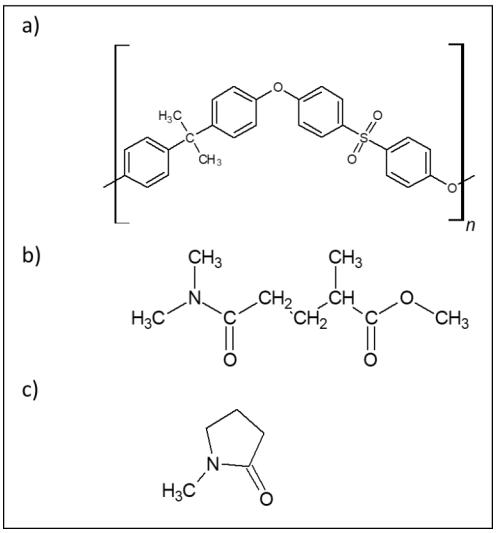

Figure1. Chemical structures of a) polysulfone polymer, b) green solvent methyl 5-(dimethylamino)-2-methyl-5-oxopentanoate (MDMO), and c) solvent N-methylpyrrolidone (NMP)

Table 1 Physicochemical properties of NMP and MDMO comparison

Characteristic	NMP	MDMO
Name	N-Methyl-2-pyrrolidone	methyl 5-(dimethylamino)-2-methyl-5-oxopentanoate
CAS No.	872-50-4	1174627-68-9
Molecular formula	C_5H_9NO	$C_9H_{17}NO_3$
Molecular weight (g mol^{-1})	99.133	187.239
Density at 25 °C (g cm^{-3})	1.028	1.043
Molar volume (cm^3/mol)	96.43	185.06
Boiling point (°C)	202	280
Flash point (°C)	95	146
Vapor pressure at 20 °C (Pa)	40	1
GHS	Danger	Warning
Toxicity	Reproductive toxicity	-

Preparation of the thin films

Polymer solutions were prepared by dissolving PSU in either MDMO or NMP at concentrations ranging from 10 to 18 wt% in 1 wt% increments. For clarity and ease of discussion, three representative PSU concentrations (12, 15, and 18 wt%) were selected. PSU was dissolved under magnetic stirring at 60 °C in MDMO and at 30 °C in NMP until complete dissolution was achieved. The time required for dissolution and homogenization depended on the PSU concentration. Subsequently, the solutions were degassed by ultrasonication for 2–4 h.

Thin films were prepared on glass plates using the doctor blade casting method. The doctor blade gap was adjusted manually to obtain a wet film thickness of 100 μm. The cast films were dried at 120 °C, with MDMO-based films requiring approximately 4 h and NMP-based films approximately 30 min. After drying, all films were readily peeled from the glass substrate by immersion in a deionized water bath.

2.2 Characterization

2.2.1 Scanning electron microscopy (SEM)

Cross-sections of all membrane samples were investigated using Nova NanoSEM 450 (FEI, USA) SEM device fitted with an SE detector. The samples were fractured in liquid nitrogen to achieve brittle fractures. Prior to SEM imaging, the samples were coated with a thin layer of gold/platinum metal alloy (60 s, argon plasma) to increase their electrical conductivity.

2.2.2 Fourier-transform infrared spectroscopy (FTIR)

FTIR spectra of all the samples were recorded using Fourier transform infrared attenuated reflectance (FTIR-ATR) on Nicolet iS5 (Thermo Fisher Scientific, USA) equipped with Ge crystal. The spectral analysis was carried out for wavenumbers from 600 to 4000 cm^{-1} at a resolution of 4 and 64 scans.

2.2.3 Thermogravimetric analysis (TGA)

The thermal stability of prepared membranes was performed by thermogravimeter TGA Q500 (TA Instruments, USA) under a nitrogen atmosphere with a flow rate of 50 mL min^{-1}. Samples of 3±1 mg were measured in temperature range from 25°C to 600°C at a heating rate of 10°C min^{-1}.

2.2.4 Viscosity measurement

The viscosity of all prepared polysulfone solutions (in MDMO or NMP) were measured using RVT model rotational viscometer (Brookfield, USA). Spindle number 4 by Brookfield was used. All measurements were provided at room temperature in volumes of 100 mL at the shear rate of 20 RPM. The measurements were repeated three times, and the average value was counted.

Intrinsic viscosity, *[η]*, was determined by measuring the viscosities of a series of PSU-based solutions of six different concentrations at laboratory temperature. The measurements were carried out using a Ubbelohde capillary viscometer. The intrinsic viscosity as well as Huggins constant (K_H) were obtained by extrapolation of experimental data according to Huggins equation (Lovell, 1989):

$$\frac{\eta_{sp}}{c} = [\eta] + K_H \cdot [\eta]^2 \cdot c \quad (1)$$

where η_{sp}/c is reduced viscosity and c is concentration.

Headspace gas chromatography (GCMS)

Headspace analysis was conducted on a Shimadzu GCMS-QP2010 Ultra device equipped with a mass detector. Rxi-5Sil M column (30 m×0.25 mm×0.25 μm, Restek) was used for separation. Helium was applied as the carrier gas at a column flow rate of 1.0 mL min^{-1}. The injection volume equaled 500 μL, the injection temperature was 300°C, and the splitless mode was used. The temperature program applied was as follows: 3 min at 50°C followed by temperature rise of 25°C min^{-1} up to 300°C held for 5 min (total time 18 min).

Samples weighing 200 mg were put into the 20 mL headspace vials. The GCMS settings comprised an incubation temperature of 40°C, a syringe temperature of 60°C, and an incubation time of 60 minutes. The mass detector conditions were EI with an ionization voltage of 70 eV, interface temperature of 320°C, ion source temperature of 230°C, and mass range of 50–350 m/z. The resultant spectra were compared with the NIST library. Each sample was measured at least twice to confirm the results.

2.2.5 Dynamic mechanical analysis (DMA)

Dynamic mechanical analysis was performed in a tension mode across a temperature range of 80-205°C and a heating rate of 3°C min^{-1} utilizing a dynamic mechanical analyzer (DMA 1, Mettler Toledo, USA). Measurements run at a frequency of 1 Hz. Before each frequency sweep measurement, an amplitude sweep scan was applied to obtain strain within the linear viscoelastic region, which was subsequently used for frequency sweep measurement.

2.2.6 Gas permeation measurements

A VAC-V1 OX2/230 (Labthink, China) equipment was used to determine the gas transmission rate through the thin films. The measurements were carried out using the time-lag method. The test conditions were: temperature 25°C, relative humidity 20%, and the gases used were carbon dioxide (CO_2), nitrogen (N_2) and oxygen (O_2). The evacuation of the test cell lasted 4 h (before each test). Thin films in the form of circular samples of 97 mm diameter deposited on filter paper circles of the same diameter were used for testing. Such samples sealed by vacuum grease were clamped between the two parts of the permeation cell. Each measurement was repeated three times. The result was obtained in the form of the gas transmission rate (GTR) of each gas used, which indicates the volume of gas in cm^3 that, under steady-state conditions, passed through a unit area of the sample (m^2) in a unit time (a day) at a unit pressure difference (0.1 MPa) and constant temperature.

Based on the known thickness of the films, the permeability for each gas was determined (Kluge et al., 2024, 2022):

$$P = GTR \cdot l = \frac{V(STP) \cdot l}{A \cdot t \cdot \Delta p} \quad (2)$$

where $V(STP)$ is the gas volume in cm^3 passing through the film at standard temperature and pressure (STP), A and l are the membrane area (cm^2) and thickness (cm), respectively, Δp is the pressure difference between the feed and permeate side of the film in cmHg and t is the time in seconds.

The values of permeability obtained from measurements can be easily converted to the commonly used Barrer unit according to the relation:

$$1\,Barrer = 10^{-10} \cdot \frac{cm^3(STP) \cdot cm}{cm^2 \cdot s \cdot cmHg} \tag{3}$$

3. Results and discussion

Figure 2 presents SEM images of fractures of two series of membranes, i.e. PSU films prepared from solutions in MNP or MDMO.

The fractures in the SEM images indicate a homogeneous, non-porous structure for all polymer concentrations and both solvents. The thicknesses of the membranes prepared from PSU solutions with the MDMO solvent ranged from 4 µm to 19 µm. The dimension strongly depended on the polymer concentration in the solution. The thicknesses of the PSU samples dissolved in NMP were also dependent on the polymer concentration and ranged from 7 µm to 15 µm. As can be seen from the graph in Figure 3B, the dependence of thickness on concentration is almost linear for PSU films prepared from solutions in NMP. Films prepared from MDMO show a sharp increase in thickness at solution concentrations above 13%. The dependence of viscosity on solution concentration shows a similar trend, as seen from the graph in Figure 3A. Thus, viscosity, just like concentration, is another parameter affecting the film thickness after the solvent evaporation.

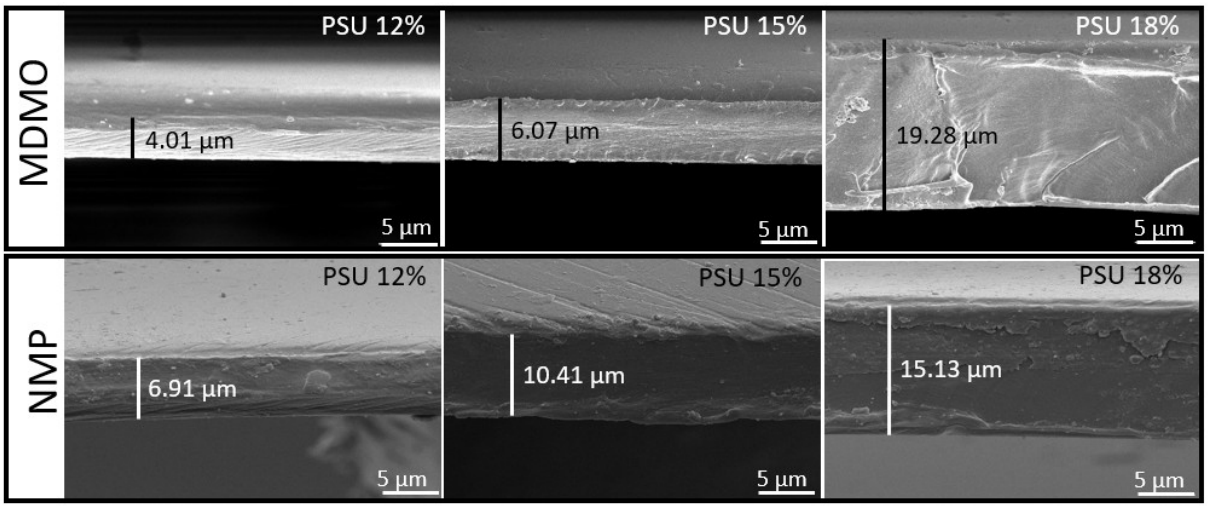

Figure 2 SEM images of the fractures of membranes prepared from polymer solutions in solvents MDMO and MNP

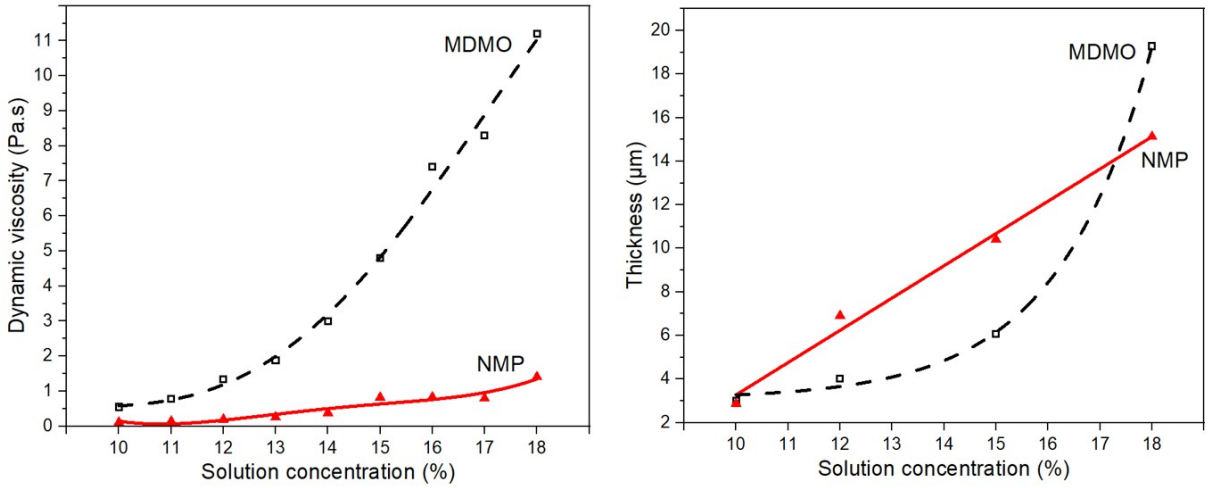

Figure 3 A) Dynamic viscosity of the PSU solutions prepared from the MDMO and MNP solvents, concentrations of PSU 10–18%; B) Dependence of thickness on concentration for PSU films prepared from solutions in NMP and MDMO

Viscosity, a property dependent on several factors such as temperature, polymer concentration, molecular weight, etc., also indicates the behavior of the polymer in solution. By determining the viscosities of dilute solutions, a concentration limit can be found below which entanglements are no longer formed. In other words, a limit between dilute and semi-dilute regimes can be found. It may be helpful to consider further processing of polymer, including casting. The first limit is defined as a critical chain overlap concentration, c^*, which is defined as $c^* = 1/[\eta]$ and physically represents the point when the concentration inside a macromolecular chain equals the solution concentration (Gupta et al., 2005). Moreover, a second critical concentration c^{**} can be defined, representing the point between a semi-dilute unentangled regime (or hydrodynamic screening regime) and a semi-dilute entangled regime. The critical concentration c^{**} differs according to literature between $1 < [\eta]c < 3$ (Gupta et al., 2005) or $1 < [\eta]c < 4$ (Hong et al., 2001). In the hydrodynamic screening region ($c^* < c < c^{**}$), the intermolecular interactions between adjacent polymer chains begin to overlap slightly, influencing the dynamic behavior of polymer chains in solution. If the concentration of the polymer solution exceeds the second critical point c^{**} the overlapping of polymer chains in the solution is noticeable, resulting in significant change of rheological behavior of the polymer solution (Hong et al., 2001). Based on the viscosity measurements, the dependence of reduced viscosity on concentration permits the determination of intrinsic viscosity (by extrapolation to zero concentration) as well as the Huggins constant (K_H), which can provide information whether the chosen solvent is a good solvent for the polymer. The Huggins constant values are around 0.3 for good solvents and in the range from 0.5 to 1 for theta solvent. Of course, it must be noted these values are invalid in both extremely diluted and highly overlapped solutions (Schoff, 1999). The results of the viscosity measurements are summarized in Table 2, including the calculated c^* and c^{**} ($[\eta]c \sim 4$). According to the Huggins constant (see Table 2), both solvents can be evaluated as good solvents for PSU. It can also be stated that both critical concentrations c^* and c^{**} are higher for MDMO-based membranes.

Table 2 Characteristics of both types of polymer solutions, as obtained from viscosity measurements

Samples	Intrinsic viscosity (L g^{-1})	Huggins constant K_H	c* (wt%)	c** (wt%)
PSU in NMP	0.0794	0.159	1.29	5.18
PSU in MDMO	0.0586	0.262	1.70	6.81

To support the conclusion from viscosity measurements of dilute polymer solutions that both solvents are good solvents for PSU, the relative energy difference (*RED*) was also calculated. The RED expresses the affinity between the polymer and the solvent based on the Hansen solubility parameters (HSP) theory. The polymer and the solvent used can be characterized by three HSPs, which represent three types of intermolecular interactions: dispersion forces (δ_d), polar forces (δ_p) and hydrogen bonding forces (δ_h). In addition, each polymer possesses an interaction radius R_0. This radius defines a 3D solubility sphere which center is defined by the three polymer solubility parameters (δ_{dp}, δ_{pp}, δ_{hp}). Each polymer/solvent pair is then assigned a distance R_a; the value of R_a can be calculated according to Equation 4.

$$R_a = \sqrt{4\left(\delta_{ds}-\delta_{dp}\right)^2+\left(\delta_{ps}-\delta_{pp}\right)^2+\left(\delta_{hs}-\delta_{hp}\right)^2} \tag{4}$$

where δ_d, δ_p, δ_h, represent the hydrogen bonding parameter, polar parameter, and dispersion parameter, and subscripts *s* and *p* refer to solvent and polymer, respectively.

The relative energy difference (*RED*), defined by Equation 5, allows to quickly determine whether the R_a of a given solvent lies inside or outside the solubility sphere of the polymer.

$$RED = R_a / R_0 \tag{5}$$

When RED is around 1 or less, the solvent can be identified as a good solvent for the polymer. The smaller the RED value, the higher the polymer solubility in the solvent. The RED greater than 1 indicates nonsolvents (AlQasas et al., 2023; Dong et al., 2018b; Matveev et al., 2024). The Hansen solubility parameters and RED for PSU and both used solvents are summarized in Table 3. The RED values for both solvents are less than 1; therefore, both NMP and MDMO can be evaluated as good solvents for PSU.

Table 3 HPSs and RED values for Ultrason S 6010 PSU and NMP and MDMO solvents (Dong et al., 2018b; Hansen, 2007; Matveev et al., 2024)

	δ_d ($MPa^{1/2}$)	δ_p ($MPa^{1/2}$)	δ_h ($MPa^{1/2}$)	R_0 ($MPa^{1/2}$)	
PSU	18.76	4.65	5.84	9.4	
	δ_d ($MPa^{1/2}$)	δ_p ($MPa^{1/2}$)	δ_h ($MPa^{1/2}$)	R_a ($MPa^{1/2}$)	RED
NMP	18.00	12.30	7.20	7.92	0.84
MDMO	15.80	10.70	9.20	9.11	0.97

An important aspect of the proper membrane function is awareness of whether any residual solvent remains in the structure, as it can act as a plasticizer under operating conditions, modifying the permeability of the membrane to certain gases (Sow Mun Lock et al., 2019). Figure 4 shows FTIR spectra for the virgin polysulfone and all films prepared, the latter reproduces the spectrum of the pure polymer well. The spectra contain aromatic C-H stretching at 1585, 1015, and 835 cm^{-1}. Characteristic absorption bands for symmetric

stretching of the sulfone group were observed at 1151 cm^{-1}, while asymmetric stretching was evident at 1322 and 1294 cm^{-1} in the spectra for PSU. Asymmetric C-O stretching was observed at 1240 and 1012 cm^{-1} (Bhattacharya et al., 2015; Singh et al., 2014; Sow Mun Lock et al., 2019).

Functional groups of MDMO and NMP are also identified in the IR spectra plotted in Figure 4. It is possible to distinctly identify a weak band at 1730 cm^{-1} corresponding to the stretching of C=O bond in the ester fragment and the region at 1640 cm^{-1} assigned to the second C=O bond as a part of the tertiary amide fragment for MDMO. This strong band appeared in all prepared membranes, indicating the presence of residual solvent. A slight coupled mode of stretching of the C-O ester bond fragment at 1060 cm^{-1} is also evident for all samples. Membranes prepared from NMP-based solutions also contain minute solvent residues, as confirmed by FTIR spectra in the region of the carbonyl stretch at 1675 cm^{-1} (Yau et al., 2015).

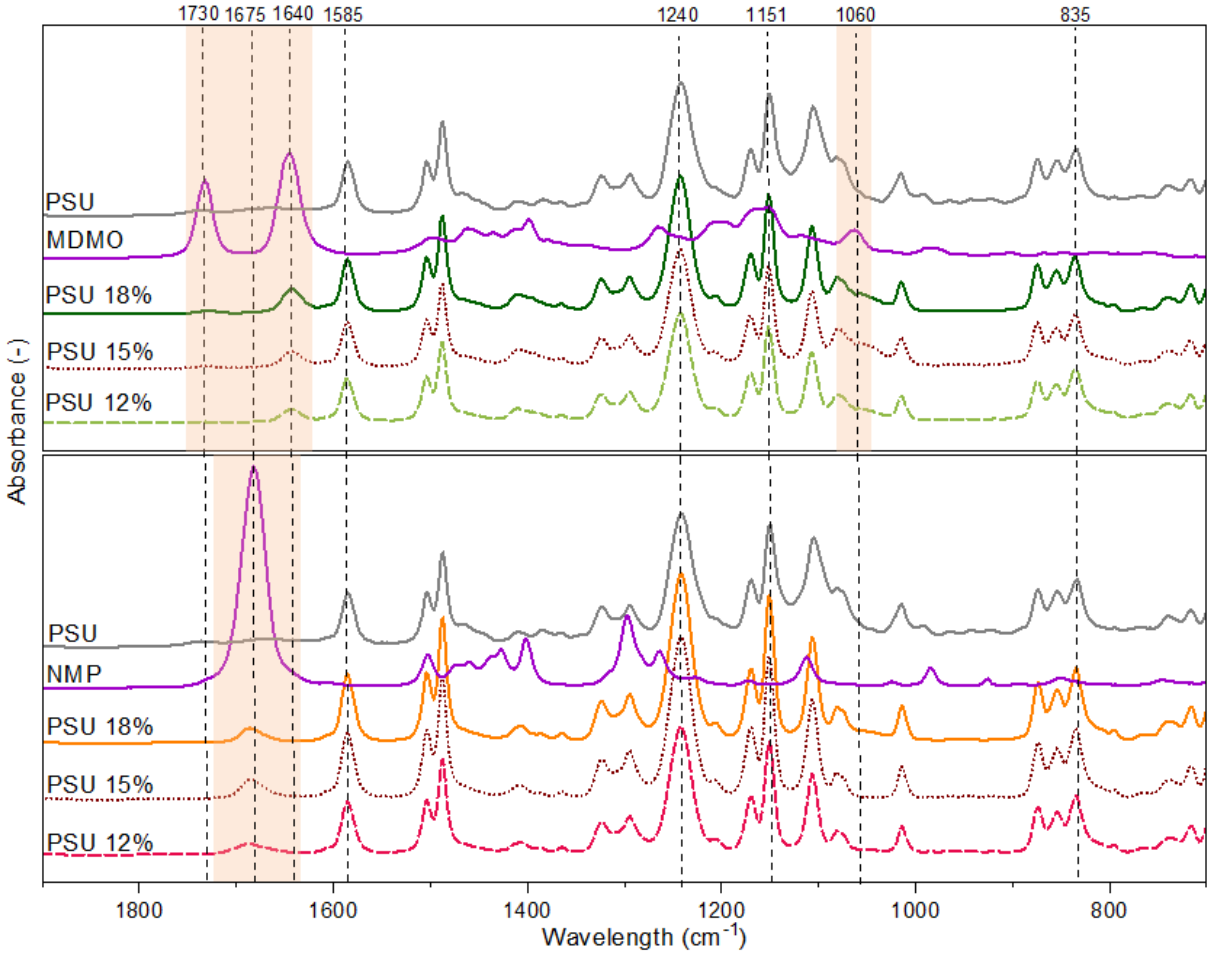

Figure 4 FTIR spectra of the virgin polymer, solvents (MDMO and NMP), and prepared solutions with concentrations of 12%, 15% and 18%

Thermogravimetric analysis (TGA) was performed to assess the amount of residual solvent in the samples and the thermal properties of the prepared membranes. The results are presented in Table 4 and graphs in Figure 5. They detail that the virgin PSU (measured on a pellet) exhibited a one-step degradation with a weight loss of 67 wt%. The polymer degradation started at around 499°C (determined as an onset temperature), and a maximum decomposition

rate was observed at 516°C (peak maximum on DTG curve). The polymer residue was almost 33 wt% upon completion of decomposition.

Based on observed data, it can be noted that both kinds of prepared membranes (based on either MDMO or NMP as the solvent) showed a two-step degradation. The first degradation step was observed in a temperature range from room temperature to 300°C. It can be assigned to the evaporation and degradation of residual solvent, which is in agreement with the results of the FTIR analysis. Moreover, this degradation step (temperature range) was also confirmed by TGA analysis of pure solvents. It can be noted that pure MDMO solvent showed higher thermal stability than NMP, although both solvents degraded almost fully before 300°C, resulting in a total weight loss of 99.6 wt% (outside the displayed data). For the MDMO-based systems, the onset of degradation was located between 136°C and 154°C, depending on the decreasing concentration of the polymer in the solution used. The NMP-based membranes exhibited a degradation onset between 118°C and 124°C for different concentrations of the polymer in the solution. As summarized in Table 4, the percentage of residual solvent in the prepared membranes is around 10–14 wt% for samples prepared from solutions in MDMO and around 8.5–12 wt% for NMP-based samples. Moreover, the weight loss corresponding to the degradation of PSU was very similar in both prepared systems (from 59 wt% to 64 wt%), which is in good agreement with the literature (Jusoh et al., 2014).

Table 4 TGA analysis of the PSU (pellet) and membranes prepared from solutions based on MDMO and NMP as the solvent at concentrations of polymer 12%, 15% and 18%

Sample	**1st decomposition**		**2nd decomposition**	
	Weight loss	**Temperature onset**	**Weight loss**	**Temperature onset**
	wt%	°C	wt%	°C
PSU	-	-	67.03	498.46
NMP	99.56	119.65	-	-
PSU 12%	11.66	123.17	60.80	482.83
PSU 15%	8.66	118.57	61.78	488.33
PSU 18%	10.41	119.10	59.30	491.17
MDMO	99.52	179.55	-	-
PSU 12%	10.95	157.56	62.45	493.68
PSU 15%	10.51	151.13	63.11	492.96
PSU 18%	14.09	136.93	63.75	488.21

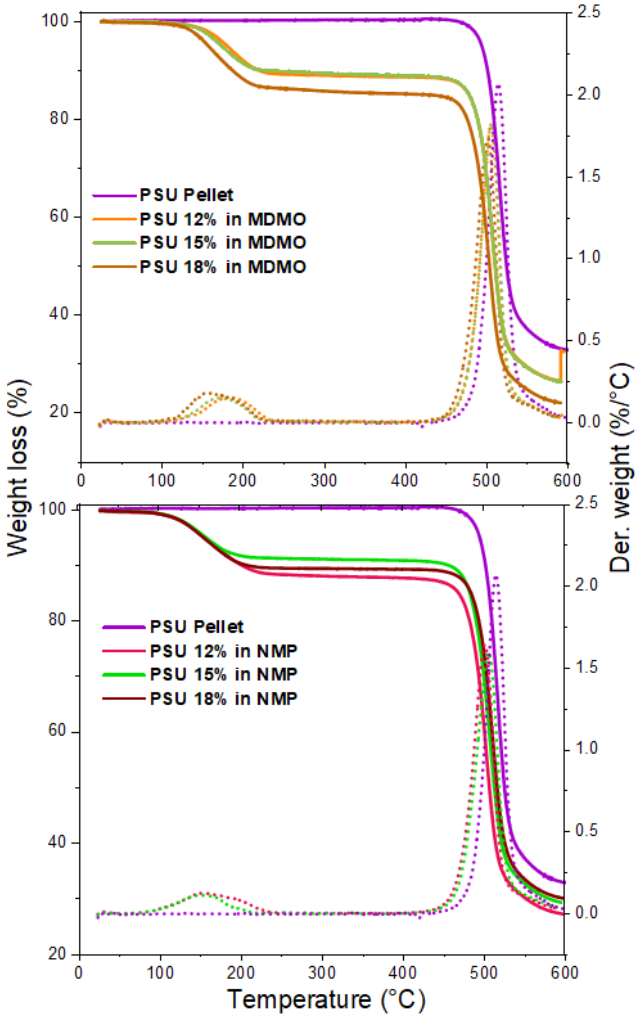

Figure 5 TGA of PSU membranes prepared from solution based on MDMO and NMP as solvents

PSU is one of the most thermally stable polymers due to its chemical structure based on a sulfonic group incorporated into a resonantly stable conjugated system with aromatic rings. The TGA results revealed that the thermal stabilities of PSU membranes containing residual solvent were almost identical to those of the virgin polymer (Molnár et al., 2005; Olmos et al., 2014).

The glass transition temperature, T_g is also an important indicator concerning the thermal properties of the membranes. Polymer-solvent interactions can significantly affect the value of T_g because the solvent acts as a plasticizer. It can lower T_g by several degrees, even at low concentrations. Changes in T_g were studied using dynamic mechanical analysis (DMA), and the results are expressed as a dependence of the loss factor tanδ on temperature (Figure 6). Membranes prepared from solutions with a PSU concentration of 18% were chosen for testing. A proportion of the samples were analyzed without further treatment, while the other samples were removed from the residual solvent by evaporating the solvents in a vacuum oven at 160°C.

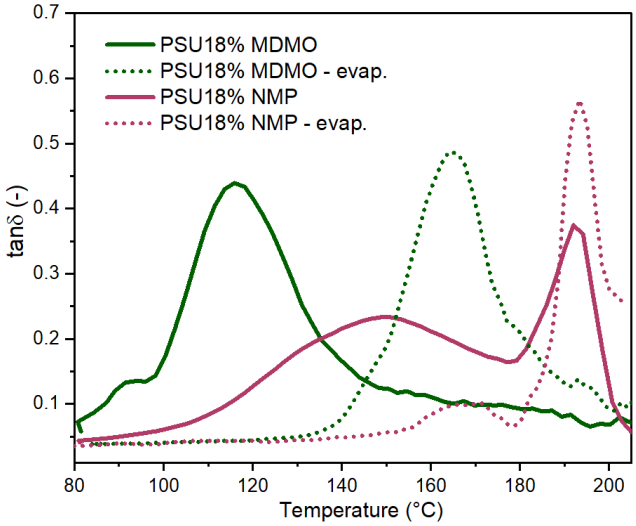

Figure 6 Dependence of tanδ on temperature as a result of DMA for untreated PSU membranes (PSU 18% MDMO and PSU 18% NMP) and vacuum oven treated membranes (PSU 18% MDMO – evap. and PSU 18% NMP - evap.)

A comparison of the DMA results revealed several interesting observations. The T_g of the NMP-based membranes remained essentially unchanged, with values of 193.4 °C for the vacuum-treated membrane and 192.6 °C for the untreated sample. However, noticeable differences were identified in the sub-T_g relaxation behavior. Specifically, the sub-T_g transition shifted from approximately 150 °C in the untreated membrane to around 170 °C after vacuum treatment. The observed increase in the sub-T_g transition temperature after solvent removal may be associated with reduced plasticization and a more constrained local chain organization. Indicating that residual NMP can affect the microstructural arrangement and local molecular dynamics of PSU, even when no significant changes are observed in the primary glass transition region.

As shown in Figure 6, the MDMO-based system exhibited a significant decrease in T_g. The sample from which the residual solvent had been removed by vacuum evaporation showed a T_g of 164.6 °C, while the untreated film exhibited a substantially lower T_g of 115.3 °C. As reflected by the Huggins constant, MDMO can penetrate between PSU chains, weaken intermolecular interactions, and enhance chain mobility, thereby significantly lowering the T_g. After vacuum treatment, the removal of residual MDMO reduced the plasticization effect and partially restored intermolecular cohesive forces between polymer chains, resulting in an increase in T_g.

Since solvent residues were identified and confirmed in the membranes, it was necessary to demonstrate their safety concerning their future use in real industrial conditions. All samples were subjected to GCMS analysis to evaluate the potential for evaporation of the residual solvent over time, i.e., during application. The results are presented in graphs in Figure 7. The dependence of absolute intensity on retention time (RT) for the pure MDMO solvent showed a dominant peak at RT 7.8 min and two smaller peaks at RT 7.26 and 7.6 min. As detailed in Figure 7, none of the graphs for the MDMO-based PSU samples contained peaks corresponding to the solvent, demonstrating the stability and safety of the prepared membranes during their application. These results are in agreement with the work of Levent Cseri et al. (Cseri and Szekely, 2019). In contrast, GCMS analysis of the NMP-based PSU

membranes revealed a peak corresponding to NMP release at RT of 5.1 min for all the samples. This could indicate a gradual release of the NMP solvent from the membrane during its use, which may represent a potential risk to the user.

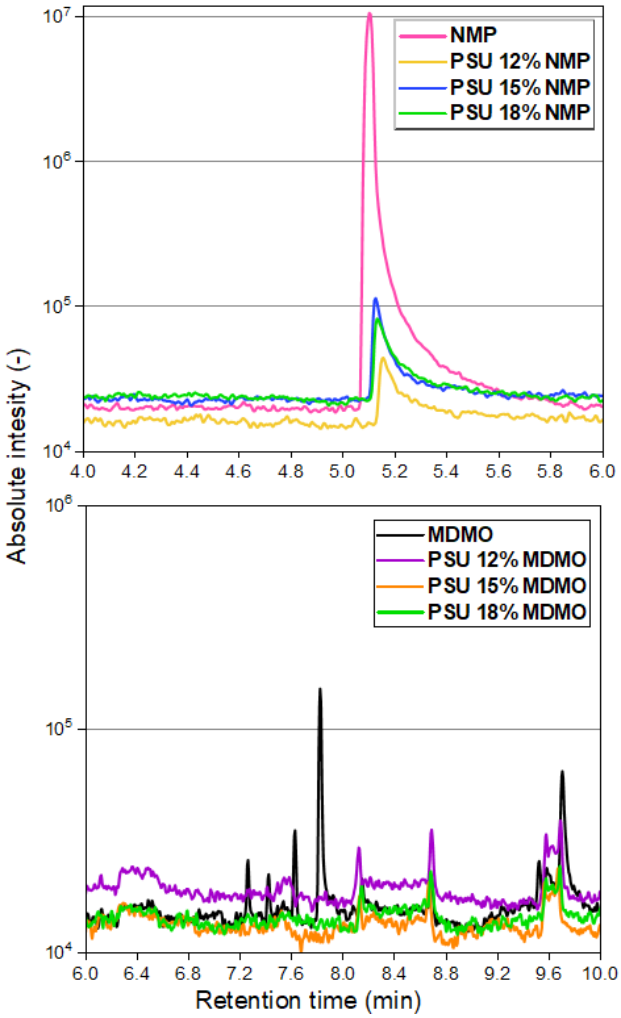

Figure 7 GCMS analysis of the pure solvents (MDMO and NMP) and membranes prepared from solutions based on these solvents

The solution-diffusion mechanism has been utilized to evaluate gas transport through PSU membranes prepared using NMP and MDMO. According to this model, the permeability (P) can be expressed as the product of the solubility (S) and the diffusivity (D) as defined by the following equation

$$P = S \cdot D \tag{6}$$

Figure 8 (A) shows the permeability of three different gases, where carbon dioxide (CO_2) exhibited higher permeability than oxygen (O_2) and nitrogen (N_2) for both membranes. The NMP-based membranes showed higher permeability, particularly for CO_2. This behavior can be attributed to the higher condensability of CO_2 and its stronger interactions with the polar sulfone groups within the polymer matrix. In contrast, O_2 and N_2 exhibited lower permeability due to their nonpolar nature and weaker interactions with the membrane material (Lin and Freeman, 2005).

It is worth noting that CO_2 permeability values reported for dense polysulfone membranes are typically in the range of 6–9 Barrer. The lower permeability observed in the present study, ~3.5 Barrer, may be related to incomplete solvent removal from the membrane matrix, as indicated by TGA.

As shown in Figure 8 (A), the MDMO-based membrane exhibited lower permeability for all tested gases compared with the NMP-based membrane, despite exhibiting lower T_g values. Lower T_g generally corresponds to increased polymer segmental mobility, which enhances free-volume fluctuations and facilitates higher gas diffusivity and permeability in polymer membranes. However, in glassy polymers such as PSU, this approach is not always straightforward. Gas transport can be influenced not only by chain mobility but also by the properties of free-volume elements and the microstructural organization of the polymer matrix *(37,38,39)*. Therefore, the lower permeability observed in the MDMO-based membrane can be correlated with solvent-induced changes in free-volume distribution and the presence of a densely packed region, which plays a pivotal role in reducing the accessibility and interconnectivity of diffusion pathways for all gases. This behavior suggests that MDMO substantially modifies the phase organization and packing structure of PSU during solvent evaporation, leading to a membrane morphology less favorable for gas transport.

While the permeability measurement describes the gas transport rate, the permselectivity provides an insight into the membrane's ability to discriminate between gases of different sizes of their molecules and interaction characteristics. The permselectivity α_{AB}, is defined by the relationship (Freeman, 1999):

$$\alpha_{AB} = P_A / P_B \tag{7}$$

where P_A is the membrane permeability for the more permeable gas and P_B for the less permeable gas.

Based on Equation 6, permselectivity can also be expressed as the product of diffusion selectivity (D_A/D_B) and solubility (S_A/S_B) selectivity:

$$\alpha_{AB} = \frac{S_A}{S_B} \cdot \frac{D_A}{D_B} \tag{8}$$

Figure 8 (B) shows that the NMP-based membrane exhibited higher selectivity for CO_2-containing gas pairs, suggesting more effective free-volume organization than the MDMO-based membrane. In contrast, the relatively low selectivity observed for the O_2/N_2 gas pair, with values approaching unity, indicates limited molecular sieving capability for both membranes. The obtained results, therefore, imply that the prepared membranes exhibited a barrier property rather than a highly selective network.

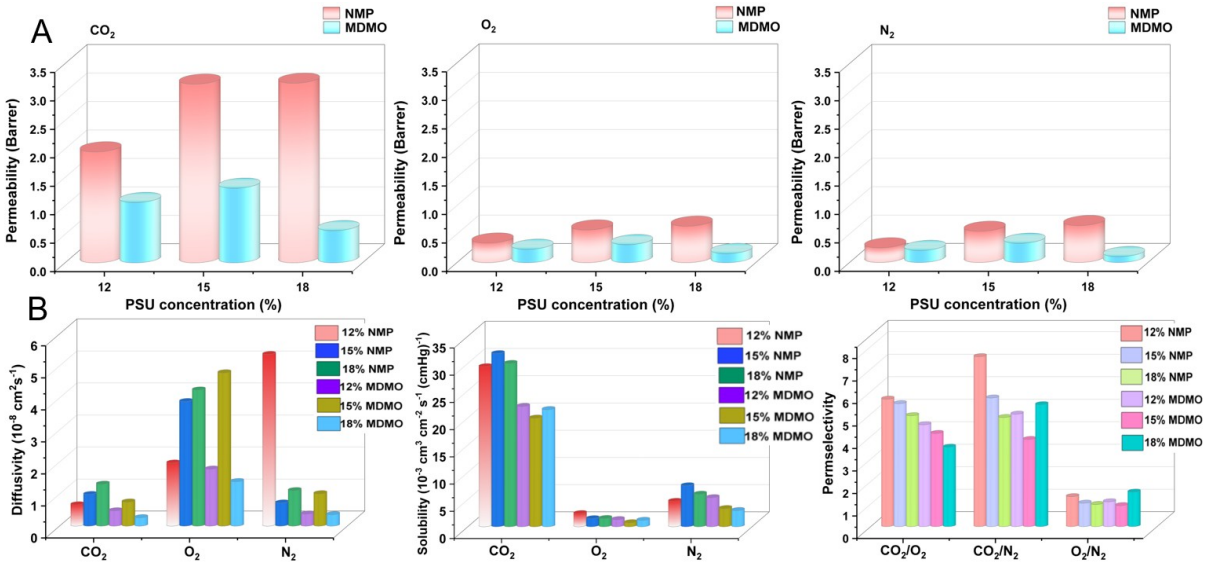

Figure 8 A) Permeability through PSU membranes based on NMP and MDMO for molecules of CO_2, N_2, and O_2, B) Solubility diffusivity permselectivity of tested PSU membranes based on NMP and MDMO

4. Conclusion

MDMO is an environmentally-friendly, non-toxic, low-volatile solvent considered a green alternative to polar aprotic solvents. In this study, MDMO was used as an alternative to N-methylpyrrolidone in PSU solutions for doctor blade cast membranes. A comparison was made of the properties of solutions of 10-18% concentration and the membranes prepared from them to investigate the effect of solvent change on the properties associated with gas separation.

The intrinsic viscosities of the solutions were measured, determining that MDMO was a good solvent for polysulfone, hence a potential alternative to NMP. However, the dynamic viscosities of the solutions with MDMO were significantly higher, indicating differences in processability and intersegmental mobility, as confirmed by values for T_g obtained by DMA. FTIR analysis revealed that both sets of membranes (based on NMP or MDMO) contained a residual solvent. TGA showed that approximately the same amount of residual solvent remained in both types of tested films, although only NMP would release gradually upon application of the membranes, as confirmed by GCMS analysis. Determining the gas transmission rates for CO_2, N_2 and O_2 demonstrated that the membranes prepared from MDMO-based solutions exhibited barrier properties.

It can be concluded that although MDMO proved to be a good solvent for PSU, the functional properties of the non-porous cast membranes made from MDMO-based solutions were rather lagging behind those where NMP was used. However, the environmentally benign solvent provides better stability to the prepared thin films, ensuring that the solvent is not released from the membrane during application. Nevertheless, it is necessary to address the lack of functional properties, which requires additivities or functionalization to maintain stability and promote the permeability and selectivity of such membranes.

Note

The authors declare no competing financial interest.

Acknowledgment

This work was supported from the Operational Programme Johannes Amos Comenius OP JAC "Application potential development in the field of polymer materials in the context of circular economy compliance (POCEK)", number CZ.02.01.01/00/23_021/0009004 and from the project DKRVO, sub-projects No. RP/CPS/2024–28/002, RP/CPS/2024–28/003, RP/CPS/2024–28/007 provided by the Ministry of Education, Youth and Sports of the Czech Republic.

References:

AlQasas, N., Eskhan, A., Johnson, D., 2023. Hansen solubility parameters from surface measurements: A comparison of different methods. Surfaces and Interfaces 36, 102594. https://doi.org/10.1016/j.surfin.2022.102594

Bhattacharya, A., Saxena, M., Sharma, S., 2015. Recycling of Polysulfone: Study Properties of Membranes. Int. J. Membrane Sci. Techno. 2, 39–46. https://doi.org/10.15379/2410-1869.2015.02.01.7

Cseri, L., Szekely, G., 2019. Towards cleaner PolarClean: efficient synthesis and extended applications of the polar aprotic solvent methyl 5-(dimethylamino)-2-methyl-5-oxopentanoate. Green Chemistry 21, 4178–4188. https://doi.org/10.1039/C9GC01958H

Dong, X., Al-Jumaily, A., Escobar, I., 2018a. Investigation of the Use of a Bio-Derived Solvent for Non-Solvent-Induced Phase Separation (NIPS) Fabrication of Polysulfone Membranes. Membranes 8, 23. https://doi.org/10.3390/membranes8020023

Dong, X., Jeong, T.J., Kline, E., Banks, L., Grulke, E., Harris, T., Escobar, I.C., 2020. Eco-friendly solvents and their mixture for the fabrication of polysulfone ultrafiltration membranes: An investigation of doctor blade and slot die casting methods. Journal of Membrane Science 614, 118510. https://doi.org/10.1016/j.memsci.2020.118510

Dong, X., Lu, D., Harris, T.A.L., Escobar, I.C., 2021. Polymers and Solvents Used in Membrane Fabrication: A Review Focusing on Sustainable Membrane Development. Membranes 11, 309. https://doi.org/10.3390/membranes11050309

Dong, X., Shannon, H.D., Escobar, I.C., 2018b. Investigation of PolarClean and Gamma-Valerolactone as Solvents for Polysulfone Membrane Fabrication, in: Cheng, H.N., Gross, R.A., Smith, P.B. (Eds.), ACS Symposium Series. American Chemical Society, Washington, DC, pp. 385–403. https://doi.org/10.1021/bk-2018-1310.ch024

EPA, 2022. EPA Finds NMP and 1-BP Present Unreasonable Risks to Human Health [WWW Document]. EPA U.S. Environmental Protection Agency. URL https://www.epa.gov/chemicals-under-tsca/epa-finds-nmp-and-1-bp-present-unreasonable-risks-human-health?utm_source=chatgpt.com

European Chemicals Agency., 2019. How to comply with REACH Restriction 71, guideline for users of NMP (1-methyl-2-pyrrolidone).

European Commission, 2020. Chemicals Strategy for Sustainability Towards a Toxic-Free Environment.

Freeman, B.D., 1999. Basis of Permeability/Selectivity Tradeoff Relations in Polymeric Gas Separation Membranes. Macromolecules 32, 375–380. https://doi.org/10.1021/ma9814548

Gupta, P., Elkins, C., Long, T.E., Wilkes, G.L., 2005. Electrospinning of linear homopolymers of poly(methyl methacrylate): exploring relationships between fiber formation, viscosity, molecular weight and concentration in a good solvent. Polymer 46, 4799–4810. https://doi.org/10.1016/j.polymer.2005.04.021

Hansen, C.M., 2007. Hansen Solubility Parameters: A User's Handbook, Second Edition, 0 ed. CRC Press. https://doi.org/10.1201/9781420006834
Hong, P.-D., Chou, C.-M., He, C.-H., 2001. Solvent effects on aggregation behavior of polyvinyl alcohol solutions. Polymer 42, 6105–6112. https://doi.org/10.1016/S0032-3861(01)00056-8
Jusoh, N., Keong, L.K., Mohd Shariff, A., 2014. Preparation and Characterization of Polysulfone Membrane for Gas Separation. AMR 917, 307–316. https://doi.org/10.4028/www.scientific.net/AMR.917.307
Keyte, I., Patton, N., Whiting, R., Corden, C., Flexman, K., Kadikis, N., Vincente, L.J., Grosu, B., 2022. Substance report - Aprotic Solvents (Project report No. June 2022), HBM4EU.
Kluge, S., Hartenauer, K., Tutuş, M., 2024. Morphology Behavior of Polysulfone Membranes Made from Sustainable Solvents. Gases 4, 133–152. https://doi.org/10.3390/gases4030008
Kluge, S., Kose, T., Tutuş, M., 2022. Tuning the Morphology and Gas Separation Properties of Polysulfone Membranes. Membranes 12, 654. https://doi.org/10.3390/membranes12070654
Lau, P.K.W., Koenig, A., 2001. Management, disposal and recycling of waste industrial organic solvents in Hong Kong. Chemosphere 44, 9–15. https://doi.org/10.1016/S0045-6535(00)00378-7
Liao, R., Guo, Y., Yang, L., Zhou, H., Jin, W., 2023. Solvent-induced microstructure of polyimide membrane to enhance CO2/CH4 separation. Journal of Membrane Science 666, 121199. https://doi.org/10.1016/j.memsci.2022.121199
Lin, H., Freeman, B.D., 2005. Materials selection guidelines for membranes that remove CO2 from gas mixtures. Journal of Molecular Structure 739, 57–74. https://doi.org/10.1016/j.molstruc.2004.07.045
Loh, C.H., Wu, B., Ge, L., Pan, C., Wang, R., 2018. High-strength N-methyl-2-pyrrolidone-containing process wastewater treatment using sequencing batch reactor and membrane bioreactor: A feasibility study. Chemosphere 194, 534–542. https://doi.org/10.1016/j.chemosphere.2017.12.013
Lovell, P.A., 1989. Dilute Solution Viscometry, in: Comprehensive Polymer Science and Supplements. Elsevier, pp. 173–197. https://doi.org/10.1016/B978-0-08-096701-1.00009-4
Maab, H., Touheed, A., 2022. Polyazole polymers membranes for high pressure gas separation technology. Journal of Membrane Science 642, 119980. https://doi.org/10.1016/j.memsci.2021.119980
Matveev, D., Anokhina, T., Raeva, A., Borisov, I., Grushevenko, E., Khashirova, S., Volkov, A., Bazhenov, S., Volkov, V., Maksimov, A., 2024. High-Performance Porous Supports Based on Hydroxyl-Terminated Polysulfone and CO2/CO-Selective Composite Membranes. Polymers 16, 3453. https://doi.org/10.3390/polym16243453
Mizrahi Rodriguez, K., Lin, S., Wu, A.X., Storme, K.R., Joo, T., Grosz, A.F., Roy, N., Syar, D., Benedetti, F.M., Smith, Z.P., 2024. Penetrant-induced plasticization in microporous polymer membranes. Chem. Soc. Rev. 53, 2435–2529. https://doi.org/10.1039/D3CS00235G
Molnár, G., Botvay, A., Pöppl, L., Torkos, K., Borossay, J., Máthé, Á., Török, T., 2005. Thermal degradation of chemically modified polysulfones. Polymer Degradation and Stability 89, 410–417. https://doi.org/10.1016/j.polymdegradstab.2005.01.031
Oh, H.J., Phillip, W.A., 2024. Polymer Physics of Separation Membranes. Macromolecules 57, 9489–9497. https://doi.org/10.1021/acs.macromol.4c02290

Olifirov, L.K., Kaloshkin, S.D., Chukov, D.I., Alexandrova, S.S., Tcherdyntsev, V.V., 2025. Study of the effect of residual N-methylpyrrolidone solvent on the physical, mechanical and thermal characteristics of molded polysulfone. Polymer Degradation and Stability 234, 111221. https://doi.org/10.1016/j.polymdegradstab.2025.111221

Olmos, D., Prolongo, S.G., González-Benito, J., 2014. Thermo-mechanical properties of polysulfone based nanocomposites with well dispersed silica nanoparticles. Composites Part B: Engineering 61, 307–314. https://doi.org/10.1016/j.compositesb.2014.01.054

Paolucci, V., D'Olimpio, G., Lozzi, L., Mio, A.M., Ottaviano, L., Nardone, M., Nicotra, G., Le-Cornec, P., Cantalini, C., Politano, A., 2020. Sustainable Liquid-Phase Exfoliation of Layered Materials with Nontoxic Polarclean Solvent. ACS Sustainable Chem. Eng. 8, 18830–18840. https://doi.org/10.1021/acssuschemeng.0c04191

Ricci, E., Minelli, M., De Angelis, M.G., 2022. Modelling Sorption and Transport of Gases in Polymeric Membranes across Different Scales: A Review. Membranes 12, 857. https://doi.org/10.3390/membranes12090857

Sarkar, A., May, R., Valmonte, Z., E. Marbella, L., 2022. PolarClean & dimethyl isosorbide: green matches in formulating cathode slurry. Energy Advances 1, 671–676. https://doi.org/10.1039/D2YA00161F

Schoff, C.K., 1999. Concentration Dependence of the Viscosity of Dilute Polymer Solutions: Huggins and Schulz-Blaschke Constants, in: Brandrup, J., Immergut, E.H., Grulke, E.A. (Eds.), The Wiley Database of Polymer Properties. Wiley. https://doi.org/10.1002/0471532053.bra053

Singh, K., Devi, S., Bajaj, H.C., Ingole, P., Choudhari, J., Bhrambhatt, H., 2014. Optical Resolution of Racemic Mixtures of Amino Acids through Nanofiltration Membrane Process. Separation Science and Technology 49, 2630–2641. https://doi.org/10.1080/01496395.2014.911023

SOLVAY, n.d. Rhodiasolv® Polarclean.

Sow Mun Lock, S., Keong Lau, K., Mohd Shariff, A., Fong Yeong, Y., Jusoh, N., 2019. Experimental Study of CO_2 Plasticization in Polysulfone Membrane for Biogas Processing, in: Rajesh Banu, J. (Ed.), Anaerobic Digestion. IntechOpen. https://doi.org/10.5772/intechopen.80957

Wang, D., Teo, W.K., Li, K., 2002. Preparation and characterization of high-flux polysulfone hollow fibre gas separation membranes. Journal of Membrane Science 204, 247–256. https://doi.org/10.1016/S0376-7388(02)00047-9

Xie, W., Tiraferri, A., Liu, B., Tang, P., Wang, F., Chen, S., Figoli, A., Chu, L.-Y., 2020. First Exploration on a Poly(vinyl chloride) Ultrafiltration Membrane Prepared by Using the Sustainable Green Solvent PolarClean. ACS Sustainable Chem. Eng. 8, 91–101. https://doi.org/10.1021/acssuschemeng.9b04287

Yau, H.C., Bayazit, M.K., Steinke, J.H.G., Shaffer, M.S.P., 2015. Sonochemical degradation of N-methylpyrrolidone and its influence on single walled carbon nanotube dispersion. Chem. Commun. 51, 16621–16624. https://doi.org/10.1039/C5CC06526G

Yong, W.F., Chung, T.-S., Weber, M., Maletzko, C., 2018. New polyethersulfone (PESU) hollow fiber membranes for CO 2 capture. Journal of Membrane Science 552, 305–314. https://doi.org/10.1016/j.memsci.2018.02.008